CFL3D with a Real-Gas Roe Solver

Hiroaki Nishikawa

February 2005

1 Introduction

In hypersonic flows, over a blunt body in particular, the air experiences very high compression through a bow shock and rapid deceleration towards the stagnation point, thus creating an extremely high-temperature region between the shock and the body. In such a flow, the temperature of the air can be high enough to violate the assumption of a perfect gas, and then we would have to consider real-gas effects (or high-temperature effects) such as chemical reactions.

In this work, assuming thermal and chemical equilibrium*, we upgrade the CFL3D for high-temperature effects. Key elements are the interface flux (a Riemann solver) and the equation of state (EOS). The flux function must be replaced by the one derived from the governing equations for a general gas, which then must be supplemented by the general EOS. Specifically, we employ the Riemann solver developed by Liou et. al [1] and the tabulated EOS constructed by Tannehill and Mugge [2].

The results show that real-gas effects are very important for a flow over a blunt body, but not at all for a body with a pointed-nose.

2 Real-Gas Roe Solver

Flux functions such as the Roe solver is derived from the Jacobian matrix,

$$\mathbf{A} = \begin{bmatrix} 0 & 1 & 0 & 0 & 0 \\ \Pi_\rho - u^2 & 2u - u\Pi_{m_x} & \Pi_{m_y} & \Pi_{m_z} & \Pi_{E_s} \\ -uv & v & u & 0 & 0 \\ -uw & w & 0 & u & 0 \\ u(\Pi_\rho - H) & H + u\Pi_{m_x} & u\Pi_{m_y} & u\Pi_{m_z} & u(1 + \Pi_{E_s}) \end{bmatrix} \tag{1}$$

of the 3D Euler equations

$$\mathbf{U}_t + \mathbf{A}\mathbf{U}_x + \mathbf{B}\mathbf{U}_y + \mathbf{C}\mathbf{U}_z = 0 \tag{2}$$

*A flow may be nonequilibrium immediately behind a shock. But it depends on the scale of the problem. For a flow around a vehicle or an airfoil that are large enough, the flow may be taken as equilibrium.

where $\mathbf{A} = \partial\mathbf{F}/\partial\mathbf{U}$,

$$\mathbf{U} = \begin{bmatrix} \rho \\ m_x \\ m_y \\ m_z \\ E_s \end{bmatrix}, \quad \mathbf{F} = \begin{bmatrix} \rho u \\ \rho u^2 + p \\ \rho uv \\ \rho uw \\ \rho uH \end{bmatrix}, \quad p = \Pi(\mathbf{U}), \quad H = \left[E_s + \Pi(\mathbf{U})\right]/\rho. \tag{3}$$

where the pressure is now calculated from the pressure function $\Pi(\mathbf{U})$, i.e. a general EOS. The Roe solver computes the flux through the cell-interface by solving the Riemann problem based on the Euler equations linearized at an average state $\hat{\mathbf{U}}$ that satisfies the Rankin-Hugoniot relation $\Delta\mathbf{F} = \mathbf{A}\Delta\hat{\mathbf{U}}$. For a perfect gas, it is possible to find such an average state (Roe-average) that is unique. In the general case, although we find the usual Roe-average for u, v, w, and H as in the perfect-gas case, one equation remains unsolved,

$$\Delta p = \hat{\Pi}_\rho \Delta\rho + \hat{\Pi}_{m_x}\Delta m_x + \hat{\Pi}_{m_y}\Delta m_y + \hat{\Pi}_{m_z}\Delta m_z + \hat{\Pi}_{E_s}\Delta E_s. \tag{4}$$

There are several approaches to deal with this relation. Here, we follow Liou et. al [1], for their method's solid theoretical basis among other methods. In [1], Liou et. al set $p = p(e, \rho)$, and introduce additional Roe-averaged values $\hat{e}$ and $\hat{\rho}$ so that (4) becomes

$$\Delta p = \hat{p}_e \Delta e + \hat{p}_\rho \Delta\rho \tag{5}$$

where $\hat{p}_e$ and $\hat{p}_\rho$ are partial derivatives that remain to be defined. Note that $\bar{p}_e = p_e(\hat{e}, \hat{\rho})$ and $\bar{p}_\rho = p_\rho(\hat{e}, \hat{\rho})$ are easily computed by some difference formula but do not satisfy (5). To define the correct average derivatives, they regard (5) as a straight line in a plane of the two average derivatives (suitably scaled), and project the easily-computable values $\bar{p}_e$ and $\bar{p}_\rho$ onto that line to define $\hat{p}_e$ and $\hat{p}_\rho$. This gives the formulas for them in terms of known averaged quantities.

Now we have all necessary average quantities $(\hat{\rho}, \hat{u}, \hat{v}, \hat{w}, \hat{H}, \hat{e}, \hat{p}_e, \hat{p}_\rho)$ to compute the dissipation term in the Roe flux function, and

$$\mathbf{F}_n = \frac{1}{2}(\mathbf{F}_R + \mathbf{F}_L) - \frac{1}{2}|\mathbf{A}_n|\Delta\mathbf{U}. \tag{6}$$

It should be understood that all quantities in the Jacobian (in the direction of normal to the ingerface) $|\mathbf{A}_n|$ are evaluated at the state $(\hat{\rho}, \hat{u}, \hat{v}, \hat{w}, \hat{H}, \hat{e}, \hat{p}_e, \hat{p}_\rho)$. For example, the average speed of sound is given by

$$\hat{a} = \sqrt{\hat{p}_\rho + \hat{p}_e(\hat{H} - \hat{e} + \hat{q}^2/2)/\hat{\rho}} \tag{7}$$

For a perfect gas, this Roe solver reduces the original Roe solver in the CFL3D which has been confirmed for several testcases. In order to complete the implementation, we need subroutines for EOS that work as $p = p(e, \rho)$ and also $e = e(p, \rho)$[†]. Here, we employ the polynomial correlations constructed for equilibrium air by Tannehill and Mugge [2].

[†]Only $p = p(e, \rho)$ is needed if there is no need to compute the energy for given pressure. In CFL3D, the variables it stores are primitive variables, and therefore we often need to compute energy from pressure. This requires a subroutine such as $e = e(p, \rho)$.

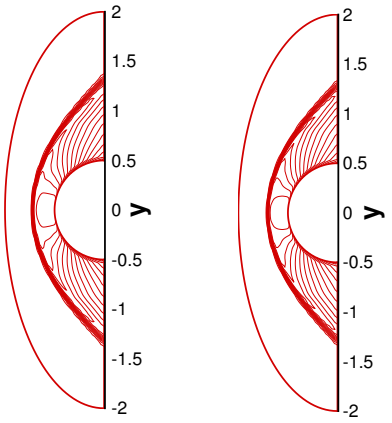

Figure 1: Mach 6, Density Contours: Perfect gas (LEFT) and Real gas (RIGHT)

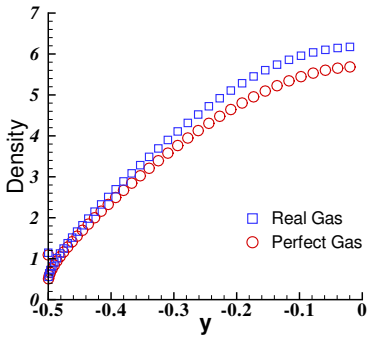

Figure 2: Mach 6, Density distribution over the lower-half of the body

3 Results

The real-gas version of the CFL3D was first run for a steady hypersonic flow with $R_e = 4.766 \times 10^6$ over a diamond airfoil for various Mach numbers up to 20, but the results were identical to those from the original CFL3D. As a second testcase, we run the code for a Mach 6 flow over a blunt body, and then we observed differences. As usually expected for real-gases, the bow shock is closer to the body(see Figure 1) and the density behind the shock is higher(see Figure 2) . These features are more pronounced in the case of Mach 8 (see Figures 3 and 4). These results show that real-gas effects are important for a flow over a rounded-nose where a rapid energy conversion takes place to raise the temperature high enough for real-gas effects, but not at all for a diamond airfoil.

4 Remarks

CFL3D breaks down for a blunt body flow with high Mach numbers (> 8), even with the perfect gas model, producing negative/infinite density. Even below Mach 8, considerable tuning (eigenvalue limiting, residual averaging, limiting, etc) was needed to make it converge to a solution.

Further tests should include a flow over an airfoil with a rounded leading edge. The code should also be tested for an unsteady flow over an oscillating airfoil to see the impact of the high-temperature effects on the unsteady behaviour of the forces and the moments.

References

[1] M.-S. Liou, B van Leer, and J.-S. Shuen, JCP, **87**, 276, 1990.

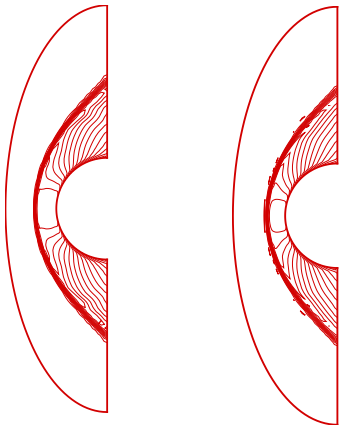

Figure 3: Mach 8, Density Contours: Perfect gas (LEFT) and Real gas (RIGHT)

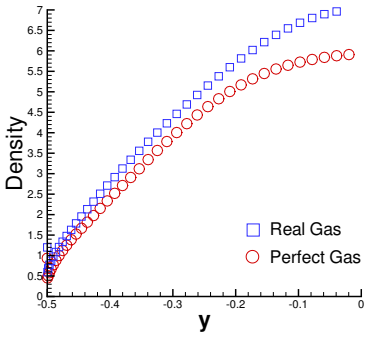

Figure 4: Mach 8, Density distribution over the lower-half of the body

[2] J. C. Tannehill and P. H. Mugge, NASA CR-2470, October 1974.

